Robotica (2009) volume 27, pp. 343–353. © 2008 Cambridge University Press
doi:10.1017/S0263574708004748 Printed in the United Kingdom

Motion analysis of a spherical mobile robot

Vrunda A. Joshi and Ravi N. Banavar*

Systems and Control Engineering, Indian Institute of Technology Bombay, Mumbai 400076, India.

(Received in Final Form: May 8, 2008. First published online: June 30, 2008)

SUMMARY

A path planning algorithm for a spherical mobile robot rolling on a plane is presented in this paper. The robot is actuated by two internal rotors that are fixed to the shafts of two motors. These are in turn mounted on the spherical shell in mutually orthogonal directions. The system is nonholonomic due to the nonintegrable nature of the rolling constraints. Further, the system cannot be converted into a chained form, and neither is it nilpotent nor differentially flat. So existing techniques of nonholonomic path planning cannot be applied directly to the system. The approach presented here uses simple geometrical notions and provides numerically efficient and intuitive solutions. We also present the dynamic model and derive motor torques for execution of the algorithm. Along the proposed paths, we achieve dynamic decoupling of the variables making the algorithm more suitable for practical applications.

KEYWORDS: Spherical mobile robot; Nonholonomic systems; Path planning of a mobile robot.

1. Introduction

The path planning of nonholonomic systems is an active area of research for the last few years. Nonholonomic constraints occur in mechanical systems either due to rolling or conservation of angular momentum. Such systems are of special interest to the robotics community due to applications like dexterous manipulation and mobile robots. These nonholonomic constraints make the path planning of these systems a challenging problem and fundamentally different than the path planning of holonomic systems. Solutions to different classes of these systems have already been provided by several researchers. Nonholonomic systems that can be reduced into a "chained form" are addressed in refs. [1] and [2]. A very elegant path planning method has been developed for nilpotentizable systems using a differential geometric approach in ref. [3]. Simple interpolation techniques can be used effectively for nonholonomic systems if they are differentially flat.[4,5] A good collection of existing path planning algorithms for nonholonomic systems can be found in ref. [6].

In this paper, we address path planning of a spherical robot rolling on a plane. The system basically consists of a sphere with a driving mechanism to roll the sphere. The nonintegrable nature of the rolling constraints renders the system nonholonomic. As compared to wheeled robots or walking robots, a spherical rolling robot offers certain advantages. The major advantage due to the spherical shape is its ability to recover from collisions and a low risk of falling down or tipping over. Different constructions have been suggested for a spherical robot. A sphere containing a universal steering wheel is described in ref. [7]. The robot by Halme *et al.*[8] consists of a single-wheeled device inside the sphere. The structure proposed by Bicchi *et al.*[9] uses a car inside the sphere as a driving mechanism. The spherical robot developed in ref. [10] uses a propulsion mechanism inside the sphere to drive the robot. The spherical robot reported in ref. [11] uses two D.C. motors to roll the sphere.

Spherical robots find wide potential applications in industry such as inspection and disaster mitigation,[12] extra-terrestrial application,[13] and child development studies.[14,15] A detailed discussion on different constructions and applications of spherical robots can be obtained from the review articles.[16,17] In spite of the wide range of applications, they are not yet popular due to the complexity involved in their path planning. The problem here is particularly difficult since the system can neither be converted into a chained form nor is it nilpotent. Since it is not differentially flat as well, all established path planning algorithms for such systems do not work for this system. The path planning of a sphere rolling on a plane has been addressed by many researchers. Brockett and Dai[18] worked on the approximate polynomial model of the system and showed that the optimal controls which optimize kinetic energy are given by elliptic functions. Jurdjevic[19] showed that the original problem is also integrable in terms of elliptic functions, and the solutions are connected to the classical problem of elastica. An iterative version of Sussman's algorithm[3] is used for optimal path planning of the spherical system studied by Bhattacharya and Agrawal.[11] In refs. [9, 20], Bicchi has shown that the mathematical model of the system can be converted into a strictly triangular structure which results in the solution of the state equations of the system. The solution can be used for path planning with other conditions like avoiding workspace limits, optimizing path with respect to the length of the path traced on the plane, and so on. All these algorithms demand excessive numerical computation at each step which seriously hinders their practical implementation. A simple and elegant path planning algorithm based on a differential geometric approach is provided in ref. [21]. In this algorithm, the sphere is reconfigured in three steps. In the first step, the desired point of contact on the plane is achieved using a trivial maneuver. In the second step, the sphere undergoes a spherical triangular

* Corresponding author. E-mail: banavar@sc.iitb.ac.in

maneuver, which is a closed trajectory on the plane, to bring the desired point on the sphere surface at the point of contact achieved in Step 1. In Step 3, the desired angle of contact is achieved by a maneuver where the point of contact travels along a latitude circle, which is a closed curve on the plane as well as on the sphere surface. The approach is more geometric and does not relate the steps to the input histories. It also assumes movement of the sphere in a single coordinate chart. Two simple and effective algorithms for reconfiguration of the sphere are given in ref. [22]. One algorithm which uses spherical trigonometric concepts is similar to the second step of the Li and Canny algorithm. Another algorithm effectively uses the final configuration of the sphere at the singularity of the ZYZ Euler angle description, thus reducing the number of configuration variables to four. It however uses control inputs in a rotating reference frame. Kiss *et al.*[5] uses the notion of differential flatness and Liouvillian properties for motion planning of hand-operated structures where the finger is a plane and the object is of a spherical shape. He has shown that if pivoting is allowed, which is the case of three inputs, the system is differentially flat and the motion planning problem can be solved using simple interpolation techniques. The flat outputs reported here are however very complicated and nonintuitive and it is difficult to proceed with the technique. If the case with two inputs is considered, the system is shown as Liouvillian and has three defect variables. The interpolation problem is then solved in the partial flat output space. Our path planning algorithm assumes the construction of the spherical robot similar to the one in ref. [11]. The kinematic model of the system is driftless with the control inputs as angular velocities along the x- and z-axes of the body frame. The path planning problem is then solved using the kinematic model developed. The proposed path planning algorithm effectively makes use of the geometry of the path traced by the sphere on the plane and reconfigures the sphere in a few steps. The algorithm is also computationally efficient. We then go on to compute the rotor torques for traversing the proposed path. For this purpose we derive the dynamic model using the Lagrange–D'Alembert equations. We observe dynamical decoupling of the states along the paths, which considerably simplifies the equations of motion. The organization of the paper is as follows: Section 2 describes the construction of the spherical mobile robot. In Section 3, the kinematic model of the system is derived. Section 4 describes the path planning algorithm proposed. In Section 5, the equations of motion are derived using Lagrange–D'Alembert principle and torque equations are obtained for execution of the motion. In Section 6, simulation results for the algorithm are reported. Section 7 provides concluding remarks.

2. Construction

The spherical robot consists of a spherical aluminium shell within which four D.C. motors are mounted symmetrically on the inner surface as shown in Fig. 1. On one axis (z-axis), two diametrically opposite motors B_1 and B_2 are mechanically coupled to rotors. Both the motors are controlled by common reversible electronic speed controller and are actuated in tandem. Similarly, on the perpendicular axis, (x-axis), two

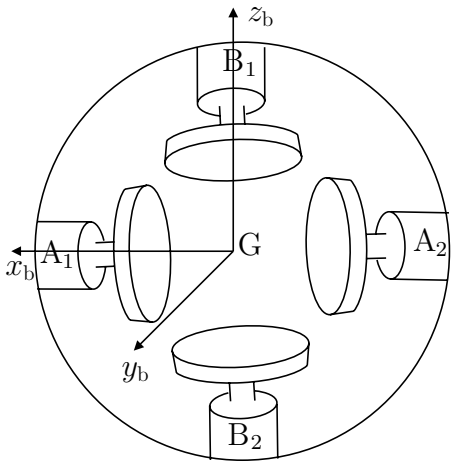

Fig. 1. Construction of the spherical robot.

motors A_1 and A_2 are attached to identical separate rotors. Both these motors are controlled by one electronic speed controller and are actuated in tandem. When both the motors on one of the axes are actuated, the corresponding rotors start rotating in one direction and the spherical shell starts rolling in the opposite direction due to conservation of angular momentum. We assume that the center of mass lies exactly at the geometric center of the sphere due to the symmetrical placing of the components. As a result of this, the spherical robot does not tend to tip over.

3. Kinematic Model

Consider a spherical robot rolling on a horizontal plane as shown in Fig. 2. An inertial coordinate frame is attached to the origin O on the plane on which the sphere is rolling and denoted by xyz. The body coordinate axes x_b, y_b, and z_b are attached to the center of the sphere at G. The set of generalized coordinates describing the sphere consists of[23]

- coordinates of the contact point I on the plane (x, y), and
- any set of variables describing the orientation of the sphere.

Orientation of the sphere is described by the ZYZ Euler angles (α, θ, ϕ). This representation suffers from singularity when $\theta = 0, \pm\pi$. Since our path passes through this singular configuration, we switch to the ZXY Euler angles (ξ, β, γ)

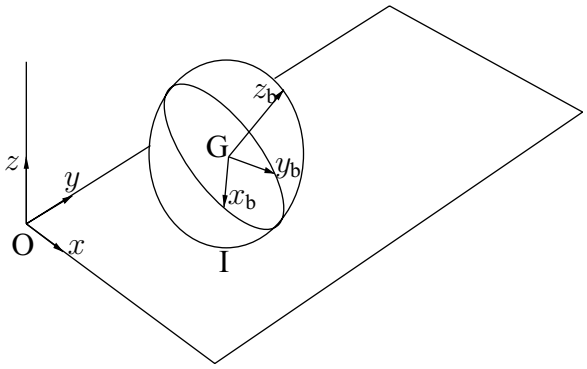

Fig. 2. Sphere rolling on a plane.

https://doi.org/10.1017/S0263574708004748 Published online by Cambridge University Press

when we encounter singularity in the ZYZ configuration. Thus we use two coordinate charts of ZYZ and ZXY Euler angle systems to form an atlas of SO(3). Let i_b, j_b, and k_b be the unit vectors along x_b-, y_b-, and z_b-axes of the body frame, respectively. Similarly let i_I, j_I, and k_I be the unit vectors along x-, y-, and z-axes of the inertial frame, respectively. For the ZYZ representation, they are related by a transformation matrix given by

$$\begin{bmatrix} i_b \\ j_b \\ k_b \end{bmatrix} = T \times \begin{bmatrix} i_I \\ j_I \\ k_I \end{bmatrix} \tag{1}$$

where

$$T = \begin{bmatrix} C_\alpha C_\theta C_\phi - S_\alpha S_\phi & S_\alpha C_\theta C_\phi + C_\alpha S_\phi & -S_\theta C_\phi \\ -C_\alpha C_\theta S_\phi - S_\alpha C_\phi & -C_\theta S_\phi S_\alpha + C_\alpha C_\phi & S_\theta S_\phi \\ C_\alpha S_\theta & S_\alpha S_\theta & C_\theta \end{bmatrix}$$

in which $S_\theta = \sin\theta$ and $C_\theta = \cos\theta$. The projection of the angular velocity of the sphere in the inertial frame is given by

$$\omega = \omega_x^I i_I + \omega_y^I j_I + \omega_z^I k_I.$$

The projection of the angular velocity vector on the inertial axes can be related to the rate of change of the Euler angles w.r.t. time using the relationship given in ref. [23]

$$\begin{bmatrix} \omega_x^I \\ \omega_y^I \\ \omega_z^I \end{bmatrix} = \begin{bmatrix} 0 \\ 0 \\ 1 \end{bmatrix} \dot\alpha + \begin{bmatrix} -S_\alpha \\ C_\alpha \\ 0 \end{bmatrix} \dot\theta + \begin{bmatrix} S_\theta C_\alpha \\ S_\theta S_\alpha \\ C_\theta \end{bmatrix} \dot\phi. \tag{2}$$

During pure rolling, the sphere moves without slipping and the rolling constraints for a sphere of radius r are given by

$$\dot x = r\omega_y^I$$
$$\dot y = -r\omega_x^I.$$

Using the expression for ω from (2) we get the no slip constraints as

$$\dot x = r(\dot\theta\cos\alpha + \dot\phi\sin\theta\sin\alpha), \tag{3a}$$
$$\dot y = r(\dot\theta\sin\alpha - \dot\phi\sin\theta\cos\alpha), \tag{3b}$$

and for a sphere of unit radius, these reduce to

$$\dot x = \dot\theta\cos\alpha + \dot\phi\sin\theta\sin\alpha, \tag{4a}$$
$$\dot y = \dot\theta\sin\alpha - \dot\phi\sin\theta\cos\alpha. \tag{4b}$$

3.1. State space model

In this section, we develop a state space model of the sphere rolling on a plane. (Without any loss of generality, we assume the sphere to have a unit radius.) Consider the angular velocity vector of the sphere along the body frame as

$$\omega = \omega_x^b i_b + \omega_y^b j_b + \omega_z^b k_b.$$

The angular velocity vector can be expressed in terms of Euler angle rates as

$$\begin{bmatrix} \omega_x^b \\ \omega_y^b \\ \omega_z^b \end{bmatrix} = \begin{bmatrix} -C_\phi S_\theta \\ S_\phi S_\theta \\ C_\theta \end{bmatrix} \dot\alpha + \begin{bmatrix} S_\phi \\ C_\phi \\ 0 \end{bmatrix} \dot\theta + \begin{bmatrix} 0 \\ 0 \\ 1 \end{bmatrix} \dot\phi. \tag{5}$$

In our system, we assume that, the control inputs are angular velocities in the body frame and therefore

$$\omega_x^b = -\dot\alpha\sin\theta\cos\phi + \dot\theta\sin\phi = u_1 \tag{6a}$$
$$\omega_y^b = \dot\alpha\sin\theta\sin\phi + \dot\theta\cos\phi = u_2 \tag{6b}$$
$$\omega_z^b = \dot\alpha\cos\theta + \dot\phi = u_3. \tag{6c}$$

Equations (4) and (6) completely describe the kinematics of the sphere giving rise to a model at the kinematic level as

$$Q\begin{bmatrix} \dot x \\ \dot y \\ \dot\alpha \\ \dot\theta \\ \dot\phi \end{bmatrix} = \begin{bmatrix} 0 \\ 0 \\ 1 \\ 0 \\ 0 \end{bmatrix} u_1 + \begin{bmatrix} 0 \\ 0 \\ 0 \\ 1 \\ 0 \end{bmatrix} u_2 + \begin{bmatrix} 0 \\ 0 \\ 0 \\ 0 \\ 1 \end{bmatrix} u_3 \tag{7}$$

where

$$Q = \begin{bmatrix} 1 & 0 & 0 & -\cos\alpha & -\sin\theta\sin\alpha \\ 0 & 1 & 0 & -\sin\alpha & \sin\theta\cos\alpha \\ 0 & 0 & -\sin\theta\cos\phi & \sin\phi & 0 \\ 0 & 0 & \sin\theta\sin\phi & \cos\phi & 0 \\ 0 & 0 & \cos\theta & 0 & 1 \end{bmatrix}.$$

We assume that the actuators can control the X and Z components of the angular velocities. We therefore set $u_2 = 0$ and the kinematic model of the system is obtained as

$$\dot x = (S_\phi C_\alpha + C_\theta S_\alpha C_\phi)u_1 + (S_\theta S_\alpha)u_3 \tag{8a}$$
$$\dot y = (-S_\phi S_\alpha + C_\theta C_\alpha C_\phi)u_1 - (S_\theta C_\alpha)u_3 \tag{8b}$$
$$\dot\alpha = (-C_\phi\,\mathrm{cosec}\,\theta)u_1 \tag{8c}$$
$$\dot\theta = (S_\phi)u_1 \tag{8d}$$
$$\dot\phi = (C_\phi\cot\theta)u_1 + u_3. \tag{8e}$$

Since we have adopted the Euler angle representation for SO(3) and these are not globally valid, we observe that the matrix Q is not invertible at $\theta = 0, \pm\pi$. These are the singular configurations of the ZYZ Euler angle description. At these configurations, model (8) is not valid and we switch to another Euler angle system. There are total 12 Euler angle systems and we have to switch to one of the Euler angle systems such that the selected system is farthest from the singularity of the ZYZ system.[24] Since the singularity in a symmetric Euler angle system cannot be avoided by switching to another symmetric Euler angle set, we have to switch to an asymmetric Euler angle system. We therefore choose the ZXY system so that patching of the two coordinate charts corresponding to the Euler angle systems ZYZ and ZXY forms an atlas for SO(3).

Consider the set of angles (ξ, β, γ) to represent the orientation of the sphere in the ZXY Euler angle system.

https://doi.org/10.1017/S0263574708004748 Published online by Cambridge University Press

The mathematical model then can be developed on similar lines to the ZYZ system as

$$\dot{x} = (-S_\beta C_\xi S_\gamma + C_\gamma S_\xi)u_1 + (S_\xi S_\gamma + S_\beta C_\gamma C_\xi)u_3 \quad (9a)$$

$$\dot{y} = (S_\beta S_\xi S_\gamma - C_\gamma C_\xi)u_1 - (C_\xi S_\gamma + S_\beta C_\gamma S_\xi)u_3 \quad (9b)$$

$$\dot{\xi} = (-S_\gamma \sec\beta)u_1 + (C_\gamma \sec\beta)u_3 \quad (9c)$$

$$\dot{\beta} = (C_\gamma)u_1 + (S_\gamma)u_3 \quad (9d)$$

$$\dot{\gamma} = (S_\gamma \tan\beta)u_1 - (C_\gamma \tan\beta)u_3. \quad (9e)$$

4. Path Planning

The path planning of the spherical mobile robot can be subdivided into two subproblems as follows:

- *Problem 1*: Given an initial configuration of the sphere as $p_0 \in \mathbb{R}^2 \times$ SO(3) and the final configuration $p_f \in \mathbb{R}^2 \times$ SO(3), determine whether a path exists between them satisfying the rolling constraints.
- *Problem 2*: Assuming that the admissible path exists between the two configurations, find such a path.

4.1. Existence of path

We need to analyze controllability of the system for proving existence of the path. We use an algorithm given in ref. [21]. The kinematic model in ZYZ-coordinate system is expressed as

$$\dot{q} = X_1(q)u_1 + X_2(q)u_3$$

where

$$q = \begin{bmatrix} x & y & \alpha & \theta & \phi \end{bmatrix}^T$$

$$X_1 = \begin{bmatrix} \sin\phi\cos\alpha + \cos\theta\sin\alpha\cos\phi \\ -\sin\phi\sin\alpha + \cos\theta\cos\alpha\cos\phi \\ -\cos\phi\,\mathrm{cosec}\,\theta \\ \sin\phi \\ \cos\phi\cot\theta \end{bmatrix}$$

$$X_2 = \begin{bmatrix} \sin\theta\sin\alpha \\ -\sin\theta\cos\alpha \\ 0 \\ 0 \\ 1 \end{bmatrix}.$$

We compute the following Lie brackets of X_1 and X_2 using the Philip Hall convention[1]

$$X_3 = [X_1, X_2]$$

$$X_4 = [X_1, X_3]$$

$$X_5 = [X_2, X_3].$$

Using these Lie brackets, we form the distribution $\triangledown = \{X_1, X_2, X_3, X_4, X_5\}$. It can be verified that $\triangledown$ is nonsingular everywhere except at the singularity of ZYZ system, i.e., $\theta = 0, \pm\pi$. We carry similar procedure for another coordinate chart using ZXY Euler angle system and verify that the distribution formed here is nonsingular everywhere except at the singularity $\beta = \pm\pi/2$. As the singularity of the two systems ZYZ and ZXY is at different points in SO(3), we patch these two coordinate systems to cover whole atlas of SO(3). Using Chow's Theorem, it can be concluded that the system is controllable and can be taken from any initial configuration to any final configuration in the configuration space $\mathbb{R}^2 \times$ SO(3).

4.2. Path planning algorithm

4.2.1. Problem statement. Consider the initial configuration $p_0 = (x_0, y_0) \times \mathcal{O}_0$ and the final configuration $p_f = (x_f, y_f) \times \mathcal{O}_f$ where $(x_i, y_i) \in \mathbb{R}^2$ and $\mathcal{O}_i \in$ SO(3). The path planning problem is to find a feasible path along which the sphere can be rolled so as to reconfigure its states from p_0 to p_f. Without any loss of generality, we assume the final configuration of the sphere to lie at the origin giving $q_f = (0, 0, 0, 0, 0)$. With this, the path planning problem is to find a feasible path along which the sphere can be rolled to move contact point of the sphere to the origin of the inertial frame with the body frame $x_b y_b z_b$ aligned with the inertial frame xyz.

4.2.2. Algorithm. The algorithm proposed here uses geometry of the path traced by the sphere on the plane making it simple and computationally efficient. We use piecewise constant inputs and switch between the two inputs for achieving reconfiguration. From an arbitrary configuration, the x_b-axis of the body frame is aligned in the horizontal plane using the input u_3 in Step 1. The z_b-axis is then aligned vertical using u_1 in Step 2. Then through a geometrical construction, the sphere is rolled along maneuvers such that it is relocated at the origin with the z_b-axis vertical. We then apply u_3 again to align the x_b- and y_b-axes with the x- and y-axes again. These steps can be explained as follows.

Step 1: Consider control input $u_1 = 0$ and $u_3 \neq 0$, then from (8) the equations are given by

$$\dot{x} = (\sin\theta\sin\alpha)u_3$$

$$\dot{y} = -(\sin\theta\cos\alpha)u_3$$

$$\dot{\alpha} = 0$$

$$\dot{\theta} = 0$$

$$\dot{\phi} = u_3.$$

It can be observed that in this maneuver, only the Euler angle ϕ changes keeping α and θ constant at α_0 and θ_0, respectively. The control input $u_3 = \dot{\phi}$ is applied till the x_b-axis is parallel to the XY plane on which the sphere is rolling. From (1), k_I component of i_b (unit vector along x_b) is zero if either $\theta = 0$ or 2π or $\phi = \pm\frac{\pi}{2}$. If $\theta_0 \neq 0$ or 2π, this can be achieved by changing the angle ϕ from ϕ_0 to either $\pi/2$ or $-\pi/2$ using the input u_3 in this step. The contact point travels along a latitude circle of radius $\sin\theta$ on the sphere surface and along a straight line on the plane as shown in Fig. 3 given by

$$x = x_0 + \sin\theta_0\sin\alpha_0 \times (\phi - \phi_0)$$

$$y = y_0 - \sin\theta_0\cos\alpha_0 \times (\phi - \phi_0).$$

https://doi.org/10.1017/S0263574708004748 Published online by Cambridge University Press

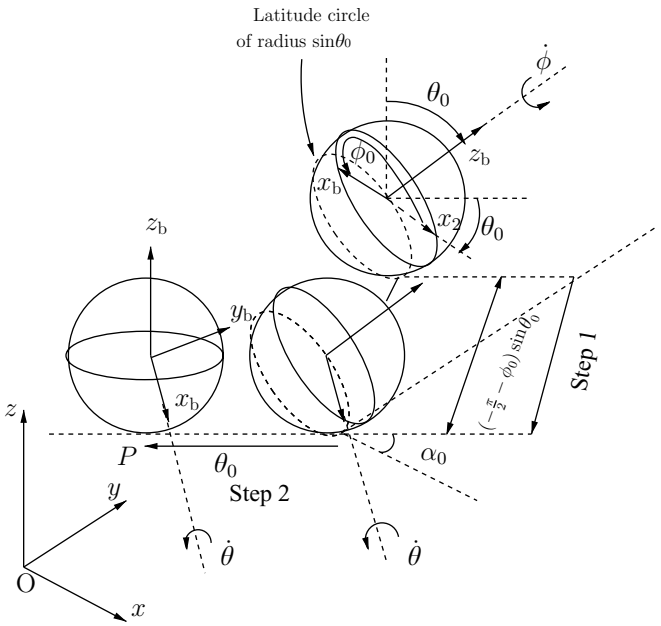

Fig. 3. Motion of the sphere : Steps 1 and 2.

When the angle ϕ changes from ϕ_0 to $\pm\pi/2$, the contact point reaches the position given by

$$\left.\begin{aligned} x_1 &= x_0 + \sin\theta_0 \sin\alpha_0 \times \left(\frac{\pi}{2} - \phi_0\right) \\ y_1 &= y_0 - \sin\theta_0 \cos\alpha_0 \times \left(\frac{\pi}{2} - \phi_0\right) \end{aligned}\right\} \quad \text{for } 0 \le \phi_0 \le \pi$$

$$\left.\begin{aligned} x_1 &= x_0 + \sin\theta_0 \sin\alpha_0 \times \left(-\frac{\pi}{2} - \phi_0\right) \\ y_1 &= y_0 - \sin\theta_0 \cos\alpha_0 \times \left(-\frac{\pi}{2} - \phi_0\right) \end{aligned}\right\} \quad \text{for } \pi \le \phi_0 \le 2\pi.$$

At the end of this maneuver, the configuration of the sphere is given by $q_1 = (x_1, y_1, \alpha_0, \theta_0, \pm\frac{\pi}{2})$.

Step 2: During this step since x_b-axis is parallel to the XY plane, the sphere can be rolled about x_b-axis using input u_1 so that the z_b-axis becomes vertical (perpendicular to the XY plane on which the sphere is rolling). This can be achieved by changing θ from θ_0 to 0 or 2π. Setting $u_3 = 0$, $u_1 \neq 0$, $\phi = \pm\pi/2$, and $\alpha = \alpha_0$ in model (8) the equations are given as

$$\left.\begin{aligned} \dot{x} &= \pm(\cos\alpha_0)u_1 \\ \dot{y} &= \mp(\sin\alpha_0)u_1 \\ \dot{\alpha} &= 0 \\ \dot{\theta} &= \pm u_1 \\ \dot{\phi} &= 0 \end{aligned}\right\} \quad \text{for } \phi = \pm\pi/2.$$

It can be observed that the angles α and ϕ do not change in this maneuver. Only the angle θ changes from θ_0 to 0 or 2π aligning z_b-axis vertical. The contact point travels along a straight line as shown in Fig. 3 given by

$$x = x_1 + \cos\alpha_0 \times (\theta - \theta_0)$$
$$y = y_1 - \sin\alpha_0 \times (\theta - \theta_0).$$

When θ changes from θ_0 to 0 or 2π, the contact point reaches the position given by

$$\left.\begin{aligned} x_2 &= x_1 - \cos\alpha_0 \times \theta_0 \\ y_2 &= y_1 + \sin\alpha_0 \times \theta_0 \end{aligned}\right\} \quad \text{for } 0 < \theta_0 \le \pi$$

$$\left.\begin{aligned} x_2 &= x_1 + \cos\alpha_0 \times (2\pi - \theta_0) \\ y_2 &= y_1 - \sin\alpha_0 \times (2\pi - \theta_0) \end{aligned}\right\} \quad \text{for } \pi \le \theta_0 < 2\pi.$$

At the end of this maneuver, the configuration of the sphere is given by $q_2 = (x_2, y_2, \alpha_0, 0, \pm\frac{\pi}{2})$. Figure 3 shows how the sphere rolls in Steps 1 and 2. As the angle ϕ_0 is in the range $\pi \le \phi_0 \le 2\pi$, Step 1 is carried out to change the angle ϕ from ϕ_0 to $-\frac{\pi}{2}$.

Step 3: Let the point of contact at the end of Step 2 be $P = (x_2, y_2)$. If O is the origin of the inertial frame attached to the XY plane, then the geometrical construction shown in Fig. 4 helps reconfiguration of the sphere. We construct two circles, one with center P and radius $2\pi n_1$ and another with center O and radius $2\pi n_2$; $n_1, n_2 \in \mathbb{Z}$. At the point P the z_b-axis is vertical and circle centered at P and radius $2\pi n_1$ gives all possible locations where the sphere can be reconfigured with z_b-axis vertical again. Similarly, the circle centered at O and radius $2\pi n_2$ gives all possible locations where the z_b-axis will be vertical. The values of n_1 and n_2 can be suitably chosen based on the distance OP. There are two points of intersections of the two circles, L and M. The sphere can either be rolled along the line PL or along the line PM. At the end of Step 2, the z_b-axis is vertical, $\theta = 0$. This is a singular configuration for the ZYZ system. The mathematical model (8) is not valid and we switch to ZXY system and use the mathematical model (9). We obtain the transformation between the two Euler angle systems and obtain a set of ZXY Euler angles from the ZYZ Euler angle system describing the orientation of the sphere at the end of Step 2 as

$$\xi_2 = \alpha_0 \pm \pi/2; \qquad \beta_2 = 0; \qquad \gamma_2 = 0.$$

Consider the path PM such that the line PM is at an angle ζ_1 w.r.t. the inertial positive x-axis. To roll the sphere along the line PM using input u_1, the x_b-axis must be aligned

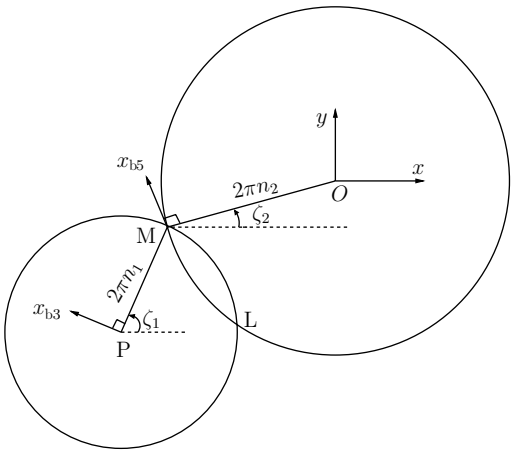

Fig. 4. Circles centered at P and O.

https://doi.org/10.1017/S0263574708004748 Published online by Cambridge University Press

perpendicular to the line PM as x_{b3} as shown in Fig. 4. This is achieved by changing the angle ξ from ξ_2 to $\xi_3 = \zeta_1 + \pi/2$ using the control input u_3. Using model (9), and the initial conditions $x = x_2,\ y = y_2,\ \xi = \xi_2,\ \beta_2 = 0,\ \gamma_2 = 0$ and control $u_1 = 0, u_3 \neq 0$, we obtain

$$\dot{x} = 0$$
$$\dot{y} = 0$$
$$\dot{\xi} = u_3$$
$$\dot{\beta} = 0$$
$$\dot{\gamma} = 0.$$

This is pivoting as expected and the contact point does not move giving $x_3 = x_2$ and $y_3 = y_2$. The angles β and γ are also unchanged giving $\beta_3 = \beta_2 = 0$ and $\gamma_3 = \gamma_2 = 0$. Only the angle ξ changes from ξ_2 to ξ_3 aligning the x_b-axis perpendicular to the line PM. We continue with our analysis using the ZXY model (9) in Steps 4–7 also.

Step 4: In this step, the sphere is rolled along the line PM using the control input u_1. With $\xi = \xi_3 = \zeta_1 + \pi/2$, $\beta_3 = 0$, $\gamma_3 = 0$, $u_1 \neq 0$, and $u_3 = 0$, we get the following equations from model (9):

$$\dot{x} = \sin\left(\zeta_1 + \frac{\pi}{2}\right)u_1 = (\cos\zeta_1)u_1$$
$$\dot{y} = -\cos\left(\zeta_1 + \frac{\pi}{2}\right)u_1 = (\sin\zeta_1)u_1$$
$$\dot{\xi} = 0$$
$$\dot{\beta} = u_1$$
$$\dot{\gamma} = 0.$$

As the angle β varies from 0 to $2\pi n_1$, the sphere rolls along a line PM given by

$$x = x_3 + \beta\cos\zeta_1$$
$$y = y_3 + \beta\sin\zeta_1.$$

At the point M the coordinates of the contact point are given by

$$x_4 = x_3 + 2\pi n_1(\cos\zeta_1)$$
$$y_4 = y_3 + 2\pi n_1(\sin\zeta_1).$$

It can be observed that during this step, only the angle β changes from 0 to $2\pi n_1$ keeping ξ and γ constant. At the end of this maneuver, the z_b-axis is vertical at the point M and the configuration of the sphere is described by $q_4 = (x_4, y_4, \xi_3, 0, 0)$.

Step 5: Control inputs $u_1 = 0$ and $u_3 \neq 0$. This step is similar to Step 3. Let the line MO be at an angle ζ_2 w.r.t. the positive inertial x-axis. In this step, the angle ξ is changed from $\zeta_1 + \pi/2$ to $\zeta_2 + \pi/2$ using the control input u_3 such that $\xi_5 = \zeta_2 + \pi/2$ and x_b-axis is aligned perpendicular to the line MO as x_{b5} as shown in Fig. 4. Similar to Step 3, this is pivoting of the sphere and its contact point does not move giving $x_5 = x_4$ and $y_5 = y_4$. At the end of this maneuver, the configuration of the sphere is described by $q_5 = (x_5, y_5, \xi_5, 0, 0)$.

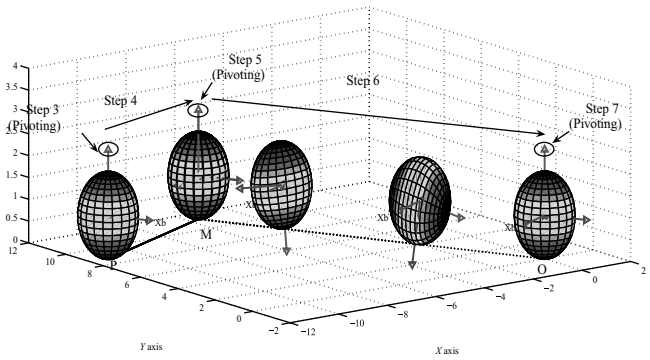

Fig. 5. Motion of the sphere : Steps 3–7.

Step 6: Control inputs $u_1 \neq 0$ and $u_3 = 0$. This step is similar to Step 4 and the sphere is rolled using the control input u_1. The contact point travels along the line MO given by

$$x = x_5 + \beta(\cos\zeta_2)$$
$$y = y_5 + \beta(\sin\zeta_2).$$

At the end of this maneuver, the contact point of the sphere reaches the point O which is origin of the inertial frame. The angles ξ and γ are unchanged giving $\xi_6 = \xi_5 = \zeta_2 + \pi/2$ and $\gamma_6 = 0$. The configuration of the sphere at the end of this maneuver is given by $q_6 = (0, 0, \xi_6, 0, 0)$.

Step 7: Control inputs $u_1 = 0$ and $u_3 \neq 0$. This is the last step of the reconfiguration. In Step 6, the sphere is rolled along the line MO and reaches origin O with z_b-axis vertical. In Step 7, we use control input u_3 and rotate the sphere about z_b-axis so as to align x_b- and y_b-axes with inertial x- and y-axes. The angle through which the sphere is rotated about the z_b-axis is given by $\xi = -\xi_6 = -(\zeta_2 + \pi/2)$. This is pivoting of the sphere using the input u_3 similar to Step 3. It can be observed that at the end of this maneuver, the sphere is reconfigured to $q_7 = (0, 0, 0, 0, 0)$. Figure 5 shows the rolling of the sphere in Steps 3–7. In Step 3, the sphere is pivoted about the z_b-axis to align the x_b-axis perpendicular to the line PM. The sphere is then rolled along the line PM using the input u_1 in Step 4. It is again pivoted about the z_b-axis in Step 5 to align the x_b-axis perpendicular to the line MO. In Step 6, it is rolled along the line MO, and in Step 7, the input u_3 is used to pivot the sphere so that the axes x_b and y_b are aligned to the inertial axes x and y, respectively.

Remark 4.1. The proposed algorithm achieves reconfiguration of the sphere from any arbitrary configuration to the origin of the configuration space. We claim that this is without loss of generality. Consider path 1 from q_0 to 0. Similarly, we have path 2 from q_f to 0. Then the path which takes the sphere from q_0 to q_f is path 1 + (path 2 in the reverse direction). In this case we can always choose the point O suitably.

https://doi.org/10.1017/S0263574708004748 Published online by Cambridge University Press

5. Dynamic Analysis

Kinematic analysis of the system plays a vital role in path planning problem. However, since we are interested in the torque histories of the motors, it is essential to develop a dynamic model of the system. In this section, we derive the equations of motion for the system using Lagrange–D'Alembert principle.[25] We introduce two new variables ψ_1 and ψ_2 for the rotor angles of X and Z rotors, respectively. The new state vector can be written as $(x, y, \alpha, \theta, \phi, \psi_1, \psi_2)$ for ZYZ Euler angle system. The sphere is assumed to be symmetrical in construction about the body axes resulting in diagonal inertia matrices for the sphere shell as well as for X and Z rotors. Let I^{s}, J^{x}, and J^{z} be the inertia matrices of the sphere, the X, and the Z rotors, respectively with respect to the body axes given by

$$I^{\mathrm{s}} = \begin{bmatrix} I^{\mathrm{s}}_{xx} & 0 & 0 \\ 0 & I^{\mathrm{s}}_{yy} & 0 \\ 0 & 0 & I^{\mathrm{s}}_{zz} \end{bmatrix}, \quad J^{\mathrm{x}} = \begin{bmatrix} J^{\mathrm{x}}_{xx} & 0 & 0 \\ 0 & J^{\mathrm{x}}_{yy} & 0 \\ 0 & 0 & J^{\mathrm{x}}_{zz} \end{bmatrix},$$

$$J^{\mathrm{z}} = \begin{bmatrix} J^{\mathrm{z}}_{xx} & 0 & 0 \\ 0 & J^{\mathrm{z}}_{yy} & 0 \\ 0 & 0 & J^{\mathrm{z}}_{zz} \end{bmatrix}.$$

Further, m is the total mass of the system, $\dot{\psi}_1 i_{\mathrm{b}}$ is the angular velocity of the X rotor, $\dot{\psi}_2 k_{\mathrm{b}}$ is the angular velocity of the Z rotor, and ω is the angular velocity of the sphere given by

$$\begin{aligned} \omega &= \omega^{\mathrm{b}}_x i_{\mathrm{b}} + \omega^{\mathrm{b}}_y j_{\mathrm{b}} + \omega^{\mathrm{b}}_z k_{\mathrm{b}} \\ &= (-\dot{\alpha} S_\theta C_\phi + \dot{\theta} S_\phi) i_{\mathrm{b}} + (\dot{\alpha} S_\theta S_\phi + \dot{\theta} C_\phi) j_{\mathrm{b}} + (\dot{\alpha} C_\theta + \dot{\phi}) k_{\mathrm{b}}. \end{aligned} \tag{10}$$

The rolling constraints for a sphere of radius r are given by

$$\dot{x} = r(\dot{\theta} \cos\alpha + \dot{\phi} \sin\theta \sin\alpha) \tag{11a}$$

$$\dot{y} = r(\dot{\theta} \sin\alpha - \dot{\phi} \sin\theta \cos\alpha). \tag{11b}$$

In the matrix form they can be written as

$$\begin{bmatrix} 1 & 0 & 0 & -r\cos\alpha & -r\sin\theta\sin\alpha & 0 & 0 \\ 0 & 1 & 0 & -r\sin\alpha & r\sin\theta\cos\alpha & 0 & 0 \end{bmatrix} \begin{bmatrix} \dot{x} \\ \dot{y} \\ \dot{\alpha} \\ \dot{\theta} \\ \dot{\phi} \\ \dot{\psi}_1 \\ \dot{\psi}_2 \end{bmatrix} = 0.$$

Define

$$a \triangleq \begin{bmatrix} a^1 \\ a^2 \end{bmatrix} = \begin{bmatrix} 1 & 0 & 0 & -r\cos\alpha & -r\sin\theta\sin\alpha & 0 & 0 \\ 0 & 1 & 0 & -r\sin\alpha & r\sin\theta\cos\alpha & 0 & 0 \end{bmatrix}.$$

Since the system is nonholonomic with rolling constraints (11a), we use Lagrange–D'Alembert principle for dynamic analysis of the system and the equations of motion for the system are given by

$$\frac{\mathrm{d}}{\mathrm{d}t}\left(\frac{\partial L}{\partial \dot{q}_i}\right) - \frac{\partial L}{\partial q_i} = \sum_{j=1}^{m} \lambda_j a^j_i + F^e_i \quad i = 1, 2, \ldots, n, \tag{12}$$

where L is Lagrangian of the system, q_i are configuration variables, F^e_i denotes the external forces acting on the system, n denotes the number of configuration variables (in our case seven), and m denotes the number of nonholonomic constraints (in our case two).

The Lagrangian can be written as

$$\begin{aligned} L = \frac{1}{2}\big[&m(\dot{x}^2 + \dot{y}^2) + (I_x)\omega^{\mathrm{b}^2}_x + (I_y)\omega^{\mathrm{b}^2}_y \\ &+ (I_z)\omega^{\mathrm{b}^2}_z + J^{\mathrm{x}}_{xx}\big(\omega^{\mathrm{b}}_x + \dot{\psi}_1\big)^2 + J^{\mathrm{z}}_{zz}\big(\omega^{\mathrm{b}}_z + \dot{\psi}_2\big)^2\big] \end{aligned}$$

where

$$I_x \triangleq I^{\mathrm{s}}_{xx} + J^{\mathrm{z}}_{xx}$$

$$I_y \triangleq I^{\mathrm{s}}_{yy} + J^{\mathrm{x}}_{yy} + J^{\mathrm{z}}_{yy}$$

$$I_z \triangleq I^{\mathrm{s}}_{zz} + J^{\mathrm{x}}_{zz},$$

and ω^{b}_x, ω^{b}_y, and ω^{b}_z are given by (6). We refer to refs. [25] and [26] for dynamic analysis of systems with internal rotors. As mentioned before, the motors transmit energy to the rotors. The coupling between the rotor dynamics and the external spherical shell causes motion of the sphere. The rate of change of the kinetic energy for the rotor is the electrical energy supplied by the motor. This appears as the two torques τ_x and τ_z in the equations corresponding to the two rotors. Appending the constraints (11) via Lagrange multipliers, we obtain the equations of motion as

$$m\ddot{x} = \lambda_1, \tag{13a}$$

$$m\ddot{y} = \lambda_2, \tag{13b}$$

$$\frac{\mathrm{d}}{\mathrm{d}t}\left(\frac{\partial L}{\partial \dot{\alpha}}\right) - \frac{\partial L}{\partial \alpha} = 0, \tag{13c}$$

$$\frac{\mathrm{d}}{\mathrm{d}t}\left(\frac{\partial L}{\partial \dot{\theta}}\right) - \frac{\partial L}{\partial \theta} = -r\lambda_1 \cos\alpha - r\lambda_2 \sin\alpha, \tag{13d}$$

$$\frac{\mathrm{d}}{\mathrm{d}t}\left(\frac{\partial L}{\partial \dot{\phi}}\right) - \frac{\partial L}{\partial \phi} = -r\lambda_1 \sin\theta \sin\alpha + r\lambda_2 \sin\theta \cos\alpha, \tag{13e}$$

$$\frac{\mathrm{d}}{\mathrm{d}t}\left(\frac{\partial L}{\partial \dot{\psi}_1}\right) - \frac{\partial L}{\partial \psi_1} = \tau_x, \tag{13f}$$

$$\frac{\mathrm{d}}{\mathrm{d}t}\left(\frac{\partial L}{\partial \dot{\psi}_2}\right) - \frac{\partial L}{\partial \psi_2} = \tau_z. \tag{13g}$$

These two Lagrange multipliers λ_1 and λ_2 are evaluated as

$$\begin{aligned} \lambda_1 &= m\ddot{x} \\ &= m\frac{\mathrm{d}}{\mathrm{d}t}(r\dot{\theta}\cos\alpha + r\dot{\phi}\sin\theta\sin\alpha) \end{aligned} \tag{14}$$

https://doi.org/10.1017/S0263574708004748 Published online by Cambridge University Press

$$\lambda_2 = m\ddot{y} = m\frac{\mathrm{d}}{\mathrm{d}t}(r\dot{\theta}\sin\alpha - r\dot{\phi}\sin\theta\cos\alpha). \quad (15)$$

Substituting the Lagrange multipliers in the equations of motion (13) and simplifying, we obtain final equations of motion as

$$\begin{aligned}
&\frac{\mathrm{d}}{\mathrm{d}t}\left[I_x\omega_x^{\mathrm{b}}\frac{\partial\omega_x^{\mathrm{b}}}{\partial\dot{\alpha}} + I_y\omega_y^{\mathrm{b}}\frac{\partial\omega_y^{\mathrm{b}}}{\partial\dot{\alpha}} + I_z\omega_z^{\mathrm{b}}\frac{\partial\omega_z^{\mathrm{b}}}{\partial\dot{\alpha}}\right.\\
&\left. + J_{xx}^{\mathrm{x}}\left(\omega_x^{\mathrm{b}} + \dot{\psi}_1\right)\times\frac{\partial\omega_x^{\mathrm{b}}}{\partial\dot{\alpha}} + J_{zz}^{\mathrm{z}}\left(\omega_z^{\mathrm{b}} + \dot{\psi}_2\right)\frac{\partial\omega_z^{\mathrm{b}}}{\partial\dot{\alpha}}\right]\\
&-\left[I_x\omega_x^{\mathrm{b}}\frac{\partial\omega_x^{\mathrm{b}}}{\partial\alpha} + I_y\omega_y^{\mathrm{b}}\frac{\partial\omega_y^{\mathrm{b}}}{\partial\alpha} + I_z\omega_z^{\mathrm{b}}\frac{\partial\omega_z^{\mathrm{b}}}{\partial\alpha}\right.\\
&\left. + J_{xx}^{\mathrm{x}}\left(\omega_x^{\mathrm{b}} + \dot{\psi}_1\right)\frac{\partial\omega_x^{\mathrm{b}}}{\partial\alpha} + J_{zz}^{\mathrm{z}}\left(\omega_z^{\mathrm{b}} + \dot{\psi}_2\right)\frac{\partial\omega_z^{\mathrm{b}}}{\partial\alpha}\right] = 0. \quad (16)
\end{aligned}$$

$$\begin{aligned}
&\frac{\mathrm{d}}{\mathrm{d}t}\left[I_x\omega_x^{\mathrm{b}}\frac{\partial\omega_x^{\mathrm{b}}}{\partial\dot{\theta}} + I_y\omega_y^{\mathrm{b}}\frac{\partial\omega_y^{\mathrm{b}}}{\partial\dot{\theta}} + I_z\omega_z^{\mathrm{b}}\frac{\partial\omega_z^{\mathrm{b}}}{\partial\dot{\theta}}\right.\\
&\left. + J_{xx}^{\mathrm{x}}\left(\omega_x^{\mathrm{b}} + \dot{\psi}_1\right)\frac{\partial\omega_x^{\mathrm{b}}}{\partial\dot{\theta}} + J_{zz}^{\mathrm{z}}\left(\omega_z^{\mathrm{b}} + \dot{\psi}_2\right)\frac{\partial\omega_z^{\mathrm{b}}}{\partial\dot{\theta}}\right]\\
&-\left[I_x\omega_x^{\mathrm{b}}\frac{\partial\omega_x^{\mathrm{b}}}{\partial\theta} + I_y\omega_y^{\mathrm{b}}\frac{\partial\omega_y^{\mathrm{b}}}{\partial\theta} + I_z\omega_z^{\mathrm{b}}\frac{\partial\omega_z^{\mathrm{b}}}{\partial\theta} + J_{xx}^{\mathrm{x}}\left(\omega_x^{\mathrm{b}} + \dot{\psi}_1\right)\right.\\
&\left.\times\frac{\partial\omega_x^{\mathrm{b}}}{\partial\theta} + J_{zz}^{\mathrm{z}}\left(\omega_z^{\mathrm{b}} + \dot{\psi}_2\right)\frac{\partial\omega_z^{\mathrm{b}}}{\partial\theta}\right] = -mr^2\ddot{\theta} - mr^2\dot{\phi}\dot{\alpha}\sin\theta. \quad (17)
\end{aligned}$$

$$\begin{aligned}
&\frac{\mathrm{d}}{\mathrm{d}t}\left[I_x\omega_x^{\mathrm{b}}\frac{\partial\omega_x^{\mathrm{b}}}{\partial\dot{\phi}} + I_y\omega_y^{\mathrm{b}}\frac{\partial\omega_y^{\mathrm{b}}}{\partial\dot{\phi}} + I_z\omega_z^{\mathrm{b}}\frac{\partial\omega_z^{\mathrm{b}}}{\partial\dot{\phi}}\right.\\
&\left. + J_{xx}^{\mathrm{x}}\left(\omega_x^{\mathrm{b}} + \dot{\psi}_1\right)\frac{\partial\omega_x^{\mathrm{b}}}{\partial\dot{\phi}} + J_{zz}^{\mathrm{z}}\left(\omega_z^{\mathrm{b}} + \dot{\psi}_2\right)\frac{\partial\omega_z^{\mathrm{b}}}{\partial\dot{\phi}}\right]\\
&-\left[I_x\omega_x^{\mathrm{b}}\frac{\partial\omega_x^{\mathrm{b}}}{\partial\phi} + I_y\omega_y^{\mathrm{b}}\frac{\partial\omega_y^{\mathrm{b}}}{\partial\phi} + I_z\omega_z^{\mathrm{b}}\frac{\partial\omega_z^{\mathrm{b}}}{\partial\phi}\right.\\
&\left. + J_{xx}^{\mathrm{x}}\left(\omega_x^{\mathrm{b}} + \dot{\psi}_1\right)\frac{\partial\omega_x^{\mathrm{b}}}{\partial\phi} + J_{zz}^{\mathrm{z}}\left(\omega_z^{\mathrm{b}} + \dot{\psi}_2\right)\frac{\partial\omega_z^{\mathrm{b}}}{\partial\phi}\right]\\
&= mr^2\dot{\theta}\dot{\alpha}\sin\theta - mr^2\ddot{\phi}\sin^2\theta - mr^2\dot{\theta}\dot{\phi}\sin\theta\cos\theta. \quad (18)
\end{aligned}$$

$$\frac{\mathrm{d}}{\mathrm{d}t}\left[J_{xx}^{\mathrm{x}}\left(\omega_x^{\mathrm{b}} + \dot{\psi}_1\right)\right] = \tau_x. \quad (19)$$

$$\frac{\mathrm{d}}{\mathrm{d}t}\left[J_{zz}^{\mathrm{z}}\left(\omega_z^{\mathrm{b}} + \dot{\psi}_2\right)\right] = \tau_z. \quad (20)$$

Equations (16)–(20) along with the rolling constraints (11) describe the dynamics of the system completely. Since we adopt the ZXY Euler angle convention as well, we develop dynamic equations using the ZXY system on similar lines.

It can be observed that the dynamics of the sphere is strongly coupled with the dynamics of the rotors and hence an explicit solution of these equations is a tough proposition. Here, we consider the proposed paths and substitute the kinematic conditions in the equations of motion, to observe the set of dynamic equations for these particular maneuvers. We observed that along these particular paths, we get dynamic decoupling of the variables giving simple torque equations which can be utilized for finding torque histories of the motor torque as follows.

Step 1: In this step, as described in Section 4.2.2, only angle ϕ changes keeping angles α and θ constant at α_0 and θ_0, respectively. Since we actuate the Z motor for this maneuver, the kinematic conditions for this step can be obtained as

$$\dot{\alpha} = 0, \quad \dot{\theta} = 0, \quad \dot{\psi}_1 = 0.$$

Applying these conditions into (6), we obtain angular velocities for this step as

$$\omega_x^{\mathrm{b}} = 0; \quad \omega_y^{\mathrm{b}} = 0; \quad \omega_z^{\mathrm{b}} = \dot{\phi}.$$

Substituting in the equations of motion (16)–(20), we get

$$\begin{aligned}
I_z\ddot{\phi} + J_{zz}^{\mathrm{z}}(\ddot{\phi} + \ddot{\psi}_2) &= -mr^2\sin^2\theta_0\ddot{\phi},\\
J_{zz}^{\mathrm{z}}(\ddot{\phi} + \ddot{\psi}_2) &= \tau_z
\end{aligned}$$

yielding

$$(I_z + mr^2\sin^2\theta_0)\ddot{\phi} = -\tau_z. \quad (21)$$

In this maneuver the sphere rolls along a latitude circle of radius $\sin\theta$. Using the parallel axis theorem, the moment of inertia about the axis z_{b}' passing through the point of contact I is $(I_z + mr^2\sin^2\theta_0)$ where I_z is the moment of inertia of the system about the z_{b}-axis. The rolling motion is instantaneous rotation of the sphere about the axis z_{b}' as shown in Fig. 6. The angular acceleration being $\ddot{\phi}$, the torque obtained in (21) can be physically interpreted.

We similarly obtain the dynamic equations for the remaining paths as follows.

Step 2: In this step, only the Euler angle θ changes and $\dot{\alpha} = 0$ and $\dot{\phi} = 0$. The angle ϕ is changed to $\pm\pi/2$ in Step 1 and only X motor actuated resulting in $\dot{\psi}_1 \neq 0$ and $\dot{\psi}_2 = 0$. Applying all these conditions in the equations of motion, a torque equation for execution of this maneuver is obtained as

$$-\tau_x = (I_x + mr^2)\ddot{\theta}.$$

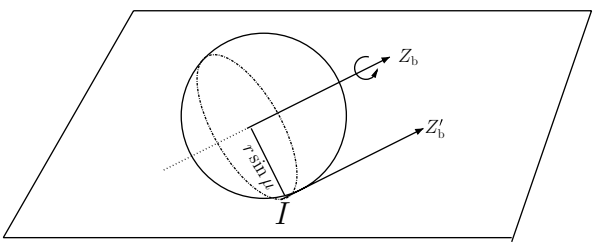

Fig. 6. Rolling about the axis z_b' in Step 1.

https://doi.org/10.1017/S0263574708004748 Published online by Cambridge University Press

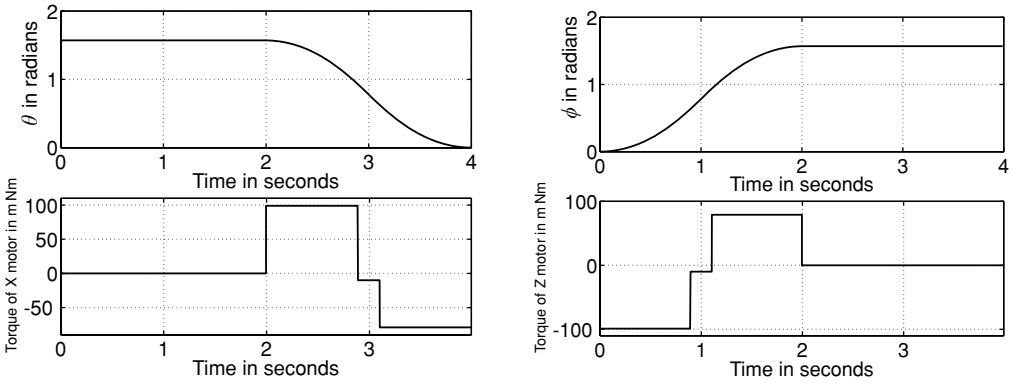

(a) Torque of X motor (b) Torque of Z motor

Fig. 7. Variation of the angle ϕ and θ in Steps 1 and 2.

Steps 3, 5, and 7: These are pivoting maneuvers and as already discussed, we use the ZXY Euler angle system from these steps. In these steps only the Euler angle ξ changes keeping β and γ unchanged. Further with the initial conditions $\beta = 0$, $\gamma = 0$ and with the Z motor activated yielding $\dot{\psi}_1 = 0$ and $\dot{\psi}_2 \neq 0$. Substituting all these conditions, a torque equation for execution of these maneuvers is obtained as

$$-\tau_z = I_z \ddot{\xi}.$$

Steps 4 and 6: In these steps the robot rolls along an equatorial circle and only angle β changes keeping ξ and γ unchanged. Since we actuate X motor for this maneuver, we have $\dot{\psi}_2 = 0$. Substituting all these conditions, a torque equation for execution of these maneuvers is obtained as

$$-\tau_x = (I_x + mr^2)\ddot{\beta}.$$

These torque equations can now be used for execution of the proposed path planning algorithm.

6. Simulation Results

Simulation of the path planning algorithm is carried out in MATLAB for reconfiguration of the sphere from the initial configuration $q_0 = (-100, 100, 0, \pi/2, 0)$ to the final configuration $q_f = (0, 0, 0, 0, 0)$ (all distances in cm and angles in radians). Figures 7, 8, and 9 show the results of the simulation. We assume the following values for the parameters:

Maximum rotor speed = 1000 rad/s,
Nominal torque = 50 m Nm,
Maximum torque = 350 m Nm,
Constant friction torque = 10 m Nm,
Maximum acceleration = 1000 rad/s^2,
Mass of the sphere(m) = 1500 g,
Radius of the robot(r) = 15 cm,
$I_{xx} = I_{yy} = I_{zz} = 225,000$ g cm^2,
$J^x_{xx} = J^z_{zz} = 1000$ g cm^2.

We consider a trapezoidal velocity profile for motion control of the two motors with equal time of acceleration and deceleration (t_a), same values for acceleration and deceleration (α), constant velocity (v) for a time (t_{cv}). For Steps 3, 5, and 7, where pivoting maneuver is used, the relation between the Euler angle and rotor angle is given by $226\ddot{\xi} = \ddot{\psi}_2$ from the simplified dynamic equations. For all other maneuvers the relation is $563.5\ddot{\xi} = \ddot{\psi}_1$.

1. In the first step, the sphere rolls from $(-100, 100)$ to $(-100, 76.43)$ on the XY plane. The angle ϕ changes from 0 to $\pi/2$. The parameters for the motion profile are $t_a = 0.894$ s, $t_{cv} = 0.211$ s, and $v = 800$ rad/s.

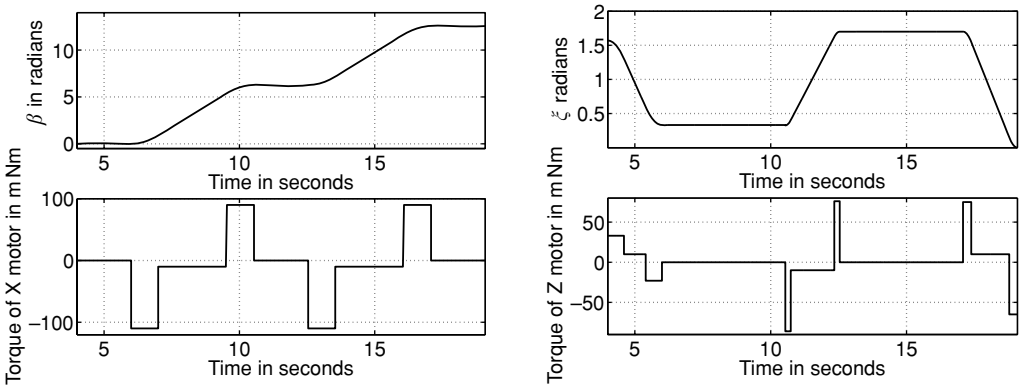

(a) Torque of X motor (b) Torque of Z motor

Fig. 8. Variation of the angle β and ξ in Steps 3–7.

https://doi.org/10.1017/S0263574708004748 Published online by Cambridge University Press

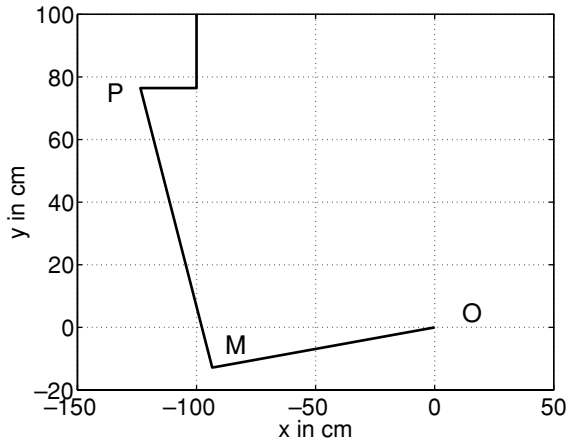

Fig. 9. Path traced on the XY plane.

2. In Step 2, the angle θ changes from $\pi/2$ to 0 bringing the sphere at the point P $= (-123.56, 76.43)$. The angle α is unchanged in Steps 1 and 2. Here, the parameters used for the motion profile are same as Step 1.
3. In Step 3, we switch over to ZXY Euler angle system with $\xi_2 = \pi/2$, $\beta_2 = \gamma_2 = 0$. In this step, the angle ξ is changed from $\pi/2$ to 0.3262^c so that the x_b-axis is perpendicular to the line PM. The parameters for the motion profile are $t_a = 0.6$ s, $t_{cv} = 0.8$ s, and $v = 200$ rad/s.
3. The sphere is then rolled along the line PM by changing β from 0 to 2π in Step 4. The parameters for the motion profile are $t_a = 1$ s, $t_{cv} = 2.54$ s, and $v = 1000$ rad/s.
4. In Step 5, the angle ξ is changed from 0.3262^c to 1.7^c to align the x_b-axis perpendicular to the line MO. The parameters for the motion profile are $t_a = 0.2$ s, $t_{cv} = 1.6$ s, and $v = 172.48$ rad/s.
5. The sphere is rolled along the line MO by changing the angle β from 0 to 2π in Step 6. The parameters for the motion profile are $t_a = 1$ s, $t_{cv} = 2.54$ s, and $v = 1000$ rad/s.
6. Step 7 aligns x_b and y_b to x and y by rotating it about the z-axis. The parameters for the motion profile are $t_a = 0.3$ s, $t_{cv} = 1.4$ s, and $v = 226$ rad/s.

Note that the angle β in Fig. 8 changes from 0 to 12.56^c which is integer multiple of 2π, equivalent to $\beta = 0$. The Z motor is actuated for Steps 1, 3, 5, and 7, while the X motor is actuated for Steps 2, 4, and 6.

The animation file of the proposed algorithm is available at `http://www.sc.iitb.ac.in/~banavar/Spherical-Robo-Animation1.avi`.

7. Conclusion

A simple path planning algorithm for a sphere rolling on a plane with internal actuators is presented. In each step, only one Euler angle is changed, thus making it computationally efficient. Along the proposed paths, the computation of the system variables is quite straightforward and involves elementary integration. The dynamic analysis shows decoupling of the variables along the proposed paths making it easy for practical implementation. The algorithms[11,27] work on the same structure of control inputs. But as they use the iterative version of the algorithm from ref. [3] which is applicable to nilpotent systems, it gives an approximate solution to the problem. Further, the algorithm is numerically complicated, nonintuitive, and also needs large number of steps for reconfiguration. As compared to that our algorithm is more intuitive, computationally efficient, and needs fewer steps to roll the sphere from any initial configuration to any final configuration. Issues like slip and rolling friction have not been incorporated at this stage of our work. We hope to address these issues as we begin implementation of our algorithm on the hardware in our laboratory.

Acknowledgment

The first author acknowledges the help of Prof. S. P. Bhat from the department of Aerospace Engineering, IIT, Bombay in clarifying issues regarding the dynamic modeling of the system.

References

1. R. M. Murray, Z. Li and S. S. Sastry, *A Mathematical Introduction to Robotic Manipulation* (CRC Press, Boca Raton, Florida, 1994).
2. R. M. Murray, Z. Li and S. S. Sastry, "Nonholonomic motion planning: Steering using sinusoids," *IEEE Trans. Automat. Control* **38**(5), 700–713 (1993).
3. G. Lafferriere and H. Sussman, "A Differential Geometric Approach to Motion Planning," **In**: *Nonholonomic Motion Planning* (Z. Li and J. F. Canny, eds.) (Kluwer Academic Publishers, New York, 1993) pp. 235–270.
4. M. Fliess, J. Levine, P. Martin and P. Rouchon, "Flatness and defect of nonlinear systems: Introductory theory and examples," *Int. J. Control* **61**(6), 1327–1361 (1995).
5. B. Kiss, J. Levine and B. Lantos, "On motion planning for robotic manipulation with permanent rolling contacts," *Int. J. Rob. Res.* **21**, 443–461 (May–June 2002).
6. Z. Li and J. Canny, *Nonholonomic Motion Planning* (Kluwer Academic Publishers, Boston, 1993).
7. L. Ferriere, G. Campion and B. Raucent, "Rollmobs: A new Drive System for Omnimobile Robots," *IEEE International Conference on Robotics and Automation*, Leuven, Belgium (1998) Vol. 3, pp. 1877–1882.
8. A. Halme, T. Schonberg and Y. Wang, "Motion Control of a Spherical Mobile Robot," *Proceedings of Advanced Motion Control*, Tsu-City, Japan (1996) Vol. 1, pp. 259–264.
9. A. Bicchi, A. Balluchi, D. Prattichizzo and A. Gorelli, "Introducing the Spherical: An Experimental Testbed for Research and Teaching in Nonholonomy," *International Conference on Robotics and Automation*, Albuquerque, USA (Apr. 1997) Vol. 3, pp. 2620–2625.
10. R. Mukherjee, M. A. Minor and J. T. Pukrushpan, "Simple Motion Planning Strategies for Spherobot: A Spherical Mobile Robot," *IEEE Conference on Decision and Control*, Phoenix, AZ (Dec. 1999) Vol. 3, pp. 2132–2137.
11. S. Bhattacharya and S. K. Agrawal, "Spherical rolling robot: Design and motion planning studies," *IEEE Trans. Rob. Automat.* **16**, 835–839 (Dec. 2000).
12. B. Chemel, E. Mutschler and H. Schempf, "Cyclops: Miniature Robotic Reconnaissance System," *IEEE International Conference on Robotics and Automation*, Detroit, MI (May 1999) Vol. 3, pp. 2298–2302.
13. F. Michaud, J. deLafontaine and S. Caron, "A Spherical Robot for Planetary Exploration," *International Symposium on Artificial Intelligence, Robotics and Automation in Space*, Canadian Space Agency, St-Hubert Qubec (2001).

https://doi.org/10.1017/S0263574708004748 Published online by Cambridge University Press

14. F. Michaud and S. Caron, "Roball, the rolling robot," *J. Autonom. Rob.* **12**, 211–222 (Mar. 2002).
15. F. Michaud, J. F. Laplante, H. Larouche, A. Duquette, S. Caron and D. Letourneau, "Autonomous spherical mobile robot for child development studies," *IEEE Trans. Syst. Man Cybernet.—Part A: Syst. Humans* **35**(4), 471–480 (July 2005).
16. J. Suomela and T. Ylikorpi, "Ball shaped robots: An historical overview and recent development at TKK," *Field Serv. Rob.* **25**(6), 343–354 (2006).
17. R. H. Armour and J. F. V. Vincent, "Rolling in nature and robotics: A review," *J. Bionic Eng.* **3**, 195–208 (Dec. 2006).
18. R. W. Brockett and L. Dai, "Nonholonomic Kinematics and the Role of Elliptic Functions in Constructive Controllability," **In**: *Nonholonomic Motion Planning* (Z. Li and J. F. Canny, eds.) (Kluwer Academic Publishers, New York, 1993) pp. 1–22.
19. V. Jurdjevic, "The geometry of the plate ball problem," *Arch. Ration. Mech. Anal. 124* **124**, 305–328 (1993).
20. A. Bicchi, D. Prattichizzo and S. S. Sastry, "Planning Motions of Rolling Surfaces," *IEEE Conference on Decision and Control*, New Orleans, LA (Dec. 1995) Vol. 3, pp. 2812–2817.
21. Z. Li and J. Canny, "Motion of two rigid bodies with rolling constraint," *IEEE Trans. Rob. Automat.* **6**, 62–72 (Feb. 1990).
22. R. Mukherjee, M. A. Minor and J. T. Pukrushpan, "Motion planning for a spherical mobile robot: Revisiting the classical ball-plate problem," *ASME J. Dyn. Syst., Meas. Control* **124**, 502–511 (Dec. 2002).
23. R. Roberson and R. Schwertassek, *Dynamics of Multibody Systems* (Springer-Verlag, New York, 1988).
24. P. Singla, D. Mortari and J. L. Junkins, "How to Avoid Singularity for Euler Angle set?," *2004 Space Flight Mechanics Meeting Conference*, Maui, Hawaii Paper AAS 04-190 (Feb. 2004).
25. A. M. Bloch, *Nonholonomic Mechanics and Control* (Springer-Verlag, New York, 2003).
26. P. S. Krishnaprasad, "Lie-poisson structures, dual-spin spacecraft and asymptotic stability," *J. Nonlinear Anal. Theory, Methods Appl.*, **9**(10), 1011–1035 (1985).
27. T. Li, Y. Zhang and Y. Zhang, "Approaches to Motion Planning for a Spherical Robot Based on Differential Geometric Control Theory," *World Congress on Intelligent Control and Automation*, Dalian, China (June 2006) pp. 8918–8922.

https://doi.org/10.1017/S0263574708004748 Published online by Cambridge University Press